Eulerian Particle Tracking In Bifurcating Biofluids

Clint W Wininger, Arizona State University, Tempe, AZ
Jeff J Heys, Montana State University, Bozeman, MT

Abstract

Biofluid flows in bifurcating geometries has become paramount to the medical community. When addressing inhaled particulate matter in the lungs, it is essential to have an efficient computational model. High-order elements offer the opportunity to model nanoparticle deposition in a case by case basis with moderate computer processor times. This adds insight into cancer precipitation as well as an advantageous route to designing patient specific therapeutic aerosols. This study focuses on developing high-order methods for particle tracking in the weakly turbulent flows that are common in the biological setting. High-order elements are used for direct numerical simulation in the incompressible fluid flow to fully resolve the transporting field. The advection-diffusion is then solved with similar methods to predict a deposition of passive and dilute particles. Eulerian-Eulerian particle tracking has shown a route to developing drug delivery on an individual basis with moderate computing times. The quick adaptation and interpolation between meshes offers a promising perspective that lends towards the utilization in the medical community. The scientific code, Nek5000, and the computer cluster at Arizona State University is used to demonstrate the effectiveness of the field method. Experiments at University of Arizona lend validation to the models. Extensions to Eulerian-Eulerian particle tracking methods with variable approximation orders are explored.

Introduction

Particle deposition has been explored experimentally and numerically since it represents an important problem encountered in various everyday situations. A particular problem of interest is deposition of particles in the human airway. Particles are inhaled through the extrathoracic and tracheobronchial airways and then are transported into the lower lungs. The airways are coated with moist mucus which provides a favorable surface for deposition and interaction with pulmonary tissue [1]. The inhaled particles can range from ultrafine with a diameter less than1μm to dust particles with a diameter of several hundred microns. Many of the inhaled particles, like second-hand cigarette smoke, can be toxic when they interact with the pulmonary tissue and lead to lung injuries [2]. Several studies have also indicated that the ultrafine particles may be more toxic than their larger counterparts of the same material [3, 4]. Thus, it is important to be able to accurately model the dynamics of nano-particles in complex geometries in order to properly assess the deposition location of the toxic elements as well as efficiently design therapeutic aerosols to target the injured region. Recent work has been completed in modeling nano-particles in the human airway by Choi et al. [5] using a two bifurcation realistic geometry and Zhang et al [6] with an idealized three bifurcation geometry and oral airway. Prior studies have used turbulence models for the fluid velocity field. This study focuses on using high-order spectral elements to fully resolve the velocity field and solve the convection-diffusion equations. In a domain of E spectral elements each with polynomials of degree N, the computational workload is on order EN^4 for EN degrees of freedom, and an exponential convergence rate. The high-order methods are also able to resolve a larger fraction of the resolvable modes for the resolution [7]. These benefits

lead to the opportunity resolve the velocity field through direct numeric simulations can provide a more accurate field in a complex geometry of bifurcating tubes as well as novel Eulerian-Eulerian particle tracking using variable approximation orders.

Theory

Governing Equations

The use of high-order spectral methods allows for direct numerical simulation to fully resolve the velocity field. The velocity field is calculated from the unsteady three-dimensional incompressible Navier-Stokes equations:

$$\frac{D\mathbf{v}}{Dt} = -\nabla p + (\mathrm{Re})^{-1}\Delta\mathbf{v} + \mathbf{f}, \quad \nabla\cdot\mathbf{v} = 0 \tag{1}$$

The **v** is a three-dimensional velocity vector, Re is the Reynolds number, *t* is the nondimensional time, *p* is a scaled pressure term, and **f** is a forcing function that is set to zero for this problem. The *div* **v** = 0 is the continuity constraint that enforces the incompressibility. After solving for the velocity field, the passive scalar solution that represents the particle concentration is obtained with the convection-diffusion equation:

$$\frac{\partial\mathbf{C}}{\partial t} + \mathbf{v}\cdot\nabla\mathbf{C} = (Di)\Delta\mathbf{v} \tag{2}$$

C is a scalar concentration field and *Di* is the diffusion coefficient that is assumed to be uniform throughout the domain. The particle concentration is very dilute and therefore can be treated as a passive scalar that does not affect the velocity field. Hence, the convection-diffusion equation can be treated as post-processing step to the fluid solution, and it can be solved multiple times for varying values of *Di* after the velocity field is known. Each different diffusion coefficient represents a particle with a different diameter.

Geometry and Boundary Conditions

For this work, multiple meshes were generated of the same geometry using the in-house program, Bifmesh. The geometry in figure 1 is based on the G0-G1 generations of Weibel's model A of the human lungs as used by Kleinsteuer et al. [8, 9]. The simulations are run at several different approximation orders to examine how the results converge towards a well-resolved solution of the fluid field and particle concentration, which used 1968 elements and 11^{th}-order basis functions (~2.6 million degrees of freedom).

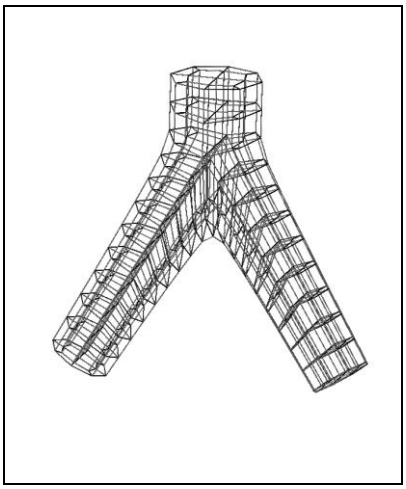

Figure 1: Single bifurcation mesh with 540 elements

The model parameters were set to approximately represent the transport of nanoparticles in the human airways. A Reynolds number of 3000 is reasonable for flow in human airways and is weakly turbulent. The diffusion coefficients range from 1.0×10^{-4} to 5.0×10^{-6} and are representative of small particles in the 1 to 10 nanometer range [6]. The inlet is defined at the top of the geometry with a velocity that is initially zero and follows a sine wave to its maximum value of 1.25 with a parabolic profile. The concentration at the inlet is constant in time defined by a parabolic cross-sectional profile with a maximum of 1.33. The outlet is at the bottom of each daughter branch and has a normal boundary condition of $p = 0$ and $du/dn = 0$. The walls of the tubes have a no-slip boundary condition in the fluid solution and zero concentration for the particle fields. The zero concentration condition allows for particles to diffuse to the walls and represents a perfect sink for particle deposition.

Numerical Methods

The Navier-Stokes equations and the convection-diffusion equation were solved using the spectral element scientific code Nek5000. Nek5000 uses Legendre spectral elements and an overlapping Schwarz preconditioner as developed by Fischer [10]. The Legendre elements use high-order polynomials to approximate the solution. The polynomials of order N introduce N-1 secondary nodes into each element (E) edge. The total nodal count for each mesh is equal to $E*N^3$ for a 3D domain. The polynomials used in this study range from 3rd to 11th order and provide great flexibility by allowing the user to change the accuracy and resolution from one trial to the next without generating a new mesh. The program allows for a variable time step that is based on a CFL condition of 0.25. The method has been used with success for determining velocity fields in similar single bifurcation biological models such as vascular flows [7] and particle fields in [11].

Each computational mesh was run at several different resolutions on the Saguaro computing cluster at Arizona State University. Using 16 Intel 64-bit Xeon EM64T CPUs connected with Infiniband high speed interconnect, the completed simulations ranged in time from 16 to 75 hours per processor depending on the number of degrees of freedom and polynomial order. For each time step, the velocity field is determined, and then the convection-

diffusion equation is solved four times to represent particles of various diameters. Since the Nek5000 code scales nearly linearly, the computation times are reported as the total number of processor hours (# of CPUs * wall clock time) necessary for task completion and is relatively independent of the number of processors used [12].

The results are examined by looking at fluid velocity/particle concentration profile across three planes through the domain (inlet, prior to bifurcation, post bifurcation). The three profiles provide a snapshot in time of the chosen quantity as it enters the domain, prior to the most computationally difficult realm, and post that same disturbance. The profiles are compared in the root-mean square error with regards to a highly resolved simulation, which uses 11^{th} order elements and contains nearly 2.6 million degrees of freedom. Results are reported as the percentage difference between the test solution and the resolved solution.

Results

In order to determine the accuracy of the Eulerian particle solution, it is imperative that the velocity field be well resolved and divergence free a priori. The initial mesh was independently refined in the order of approximation and the total number of elements. The order of approximation was allowed to range from 5 to 13, and the elements in the mesh were increased 540 up to 5952. Fast convergence of the velocity field to under 1% error is achieved for both h-and p-refinement.

Since the velocity field can be considered consistently resolved, the particle solutions can be examined independently. The solution is refined in using both p and h. The degrees of freedom range from 130,000 to 1.2 million. The nondimesionalized diffusion coefficient ranges from 10^{-4} to $5x10^{-6}$ (~1-10 nanometer particles). The solution shows good convergence to under 1% error for the largest diffusion coefficient case i.e. smallest particles, and the field with the second largest coefficient also converges but at a slightly slower rate. When the diffusion coefficient is an order of magnitude smaller (10^{-5}), the errors remain over 20% for the h-refinement but show fast convergence with p-refinement.

Since p-refinement increases the amount of interconnectedness between the computational nodes, it creates both greater accuracy and increased computational cost. Figure 2 shows total computation time for all of the simulation described previously. The error is compared for the two most advective particle solutions ($\mathfrak{D} = 1.0 \times 10^{-5}$ & 5.0×10^{-6}) since they best illustrate the accuracy differences between the simulations. Even though h-refinement results in more nodes than the p-refinement, the higher-order (p-refinement) demonstrate improved accuracy for equal simulations times of around 100 hours.

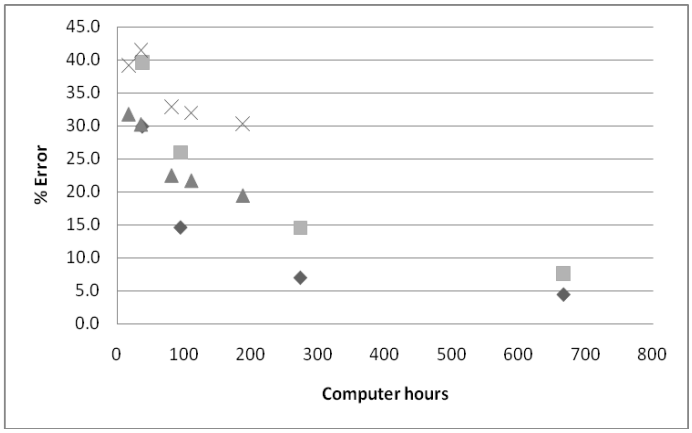

Figure 2: P-refinement demonstrates lower errors in the particle fields, $\mathfrak{D} = 1.0 \times 10^{-5}$ (◆) & $\mathfrak{D} = 5.0 \times 10^{-6}$ (■), than h-refinement, $\mathfrak{D} = 1.0 \times 10^{-5}$ (▲) & $\mathfrak{D} = 5.0 \times 10^{-6}$ (X), does at equal total computation times.

Computational Validation

Collaborators at the University of Arizona have formalized a methodology to link technetium-labeled diethylenetriamine pentaacetate (^{99m}Tc-DTPA) to second hand cigarette smoke. The research cigarettes (1R4 – University of Kentucky Tobacco and Health Research Institute) are injected with ^{99m}Tc-DTPA in four locations, and then allowed to dry for 5 minutes. Normal burn is then initiated with the smoke being drawn into a funnel in order to direct it towards a Kent Scientific small animal ventilator. The animals were prepared by anesthetizing them with a mixture of ketamine HCL (50 mg/kg body weight), xylazine (8 mg/kg body weight), and acepromazine maleate (1 mg/kg body weight). They are then placed in the ventilator with an endotracheal tube placed in the trachea 2 cm above the carina and explosed to a tidal volume of 1.5-2 mls at a respiratory rate of 60 breathes per minute [13, 14].

After the deposition is completed, each rat is placed under a gamma scanner system and observed for 10 minutes with gamma counts being recorded per 30 seconds. This verifies that the particles are securely deposited within the system, and it provides a more accurate assessment of the overall deposition in the different parts of the animal's lungs. The counts were added separately for the trachea, first bifurcation, primary airway (G2-3), and terminal airways. The deposition fraction is provided in figure 3 for the trachea (0), the first branch (1), the primary airways (2), and the terminal airways (3).

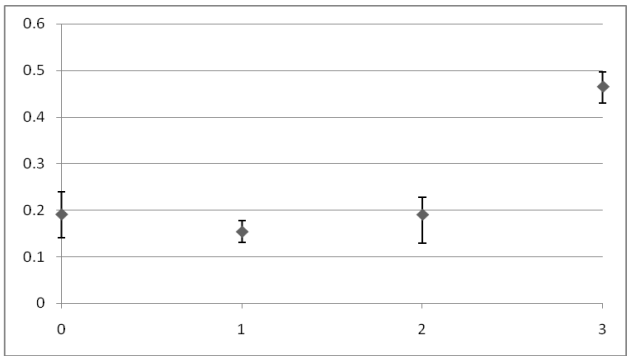

Figure 3: The deposition fraction in the trachea (0), first branch (1), primary airway (2), and the terminal airway (3) for smoke deposition in rats.

The animals in the experiments were euthanized and dissected after the gamma count observation was competed. High resolution images were taken of the entire respiratory system as well as each individual part of interest. An approximate geometry was developed by first overlying the image of first branch onto of the entire system as shown in the first frame of figure 4. This provides a very detailed image of the trachea and first generation which are most important for obtaining accurate results. A skeleton created from the cast of the lungs of a mouse was then overlaid on the image to approximate the primary and terminal airways (frame 2) [15]. Bifmesh was used similar to the prior work to develop the final three bifurcation geometry shown in figure 4.

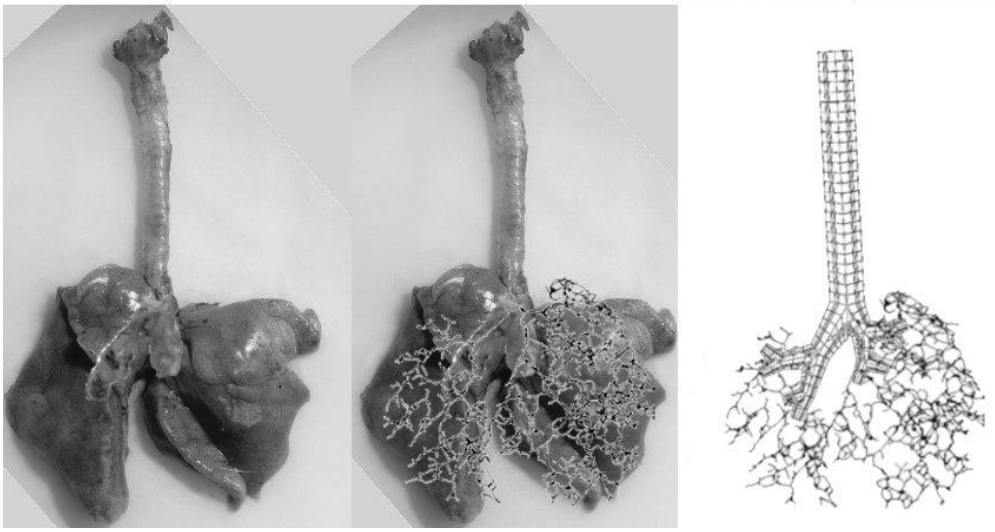

Figure 4: The computational mesh is generated based on a combination of actual rat lung images and published respiratory data [15].

Variable Approximation Orders

One of the main problems demonstrated by the previous work is that to achieve adequate resolution of an advective particle concentration, the fluid solution must be over resolved. This has no impact on the overall accuracy of the simulation, but it creates an unnecessary sacrifice of computational efficiency. This problem is caused by using the same approximation orders within the simulation for the fluid and particle fields. Interpolation can be used to generate a higher resolution solution for the particle concentration than the fluid field without generating multiple meshes or requiring multiple simulations.

The basis functions and parametric spaces used in SEM make it very inexpensive to interpolate data from one basis to another with a higher or lower approximation order. Therefore the expensive fluid problem can be solved on coarser mesh, and then the velocity data is interpolated onto finer mesh to fully resolve the less expensive particle solution. The current method utilizes $\mathbb{P}_N - \mathbb{P}_{N-2}$ spectral elements which means that the pressure is solved on a mesh that is of order N-2 while the velocity is of order N. The values of velocity and

pressure are interpolated back and forth between the Gauss-Lobatto-Legendre velocity grid and the discontinuous Gauss-Legendre pressure grid [16].

This same technique can be used to interpolate the final velocity solution onto a higher-order continuous Gauss-Lobatto-Legendre grid for solving the advection-diffusion equation. Figure 5 shows that the fluid solution requires far more computation time than the particle solution. The fluid solution requires solving the Helmholtz operator in each spatial direction as well as a very costly PCG solve of a consistent Poisson operator while the particle solution only requires a single solution to the Helmholtz operator. Therefore in the simulations shown in figure 5 (four particle sizes), the fluid solution requires 50% of the overall simulation time, and each particle solution requires less than 10%.

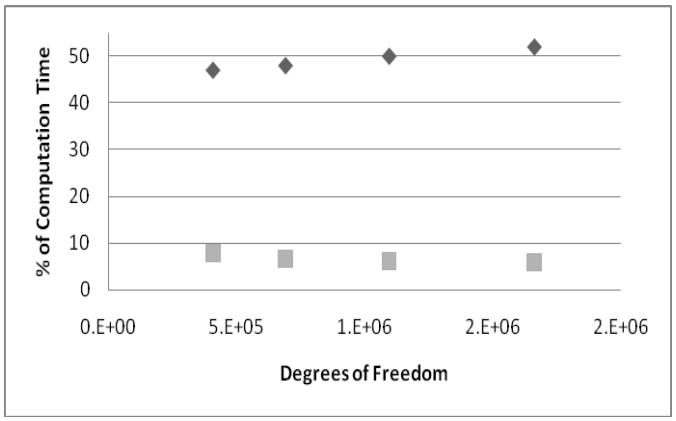

Figure 5: Converging to a solution for the consistent Poisson operator and three Helmholtz operators in the fluid solution (◆) requires over half of overall simulation time, while each of the four solves associated with Helmholtz operator in the advection-diffusion equation (■) requires less than 10% of the time.

This disparity becomes even more pronounced as the particle field becomes more advective because extremely high resolution is required to capture the high frequency waves. Solving the Navier-Stokes equations on a coarser grid becomes very appealing. Also, the stiffness of the Helmholtz operator in the particle solution is proportional to the diffusion coefficient. Therefore, as the diffusion coefficient is decreased, the solution to the advection-diffusion equation can be obtained with fewer PCG loops. The excess time for the highest resolution solutions should be somewhat mitigated by this feature.

Further, the stability of the simulation is based on the CFL condition, $\max_{\Omega}(U\Delta t/\Delta x)$. The axial node spacing can be exploited to maintain a manageable time step while still providing adequate resolution in the particle solution to prevent dispersion error oscillations. The CFL condition could still become unstable do to the decreasing Δx in the axial direction of the particle grid, but the problem can be partly circumvented using variable filter strengths for each field or subcycling [17].

The Nek5000 program will first solve the Navier-Stokes equation exactly as it did before, but then the velocity solution is interpolated onto a set of higher-order Gauss-Lobatto nodes. Two sets of basis functions are demonstrated in figure 6. The AD equation can then

be solved on the finely resolved domain. For the output steps, the particle solution is interpolated back onto the initial velocity grid. A less smooth filter can aid in stabilizing the particle solutions.

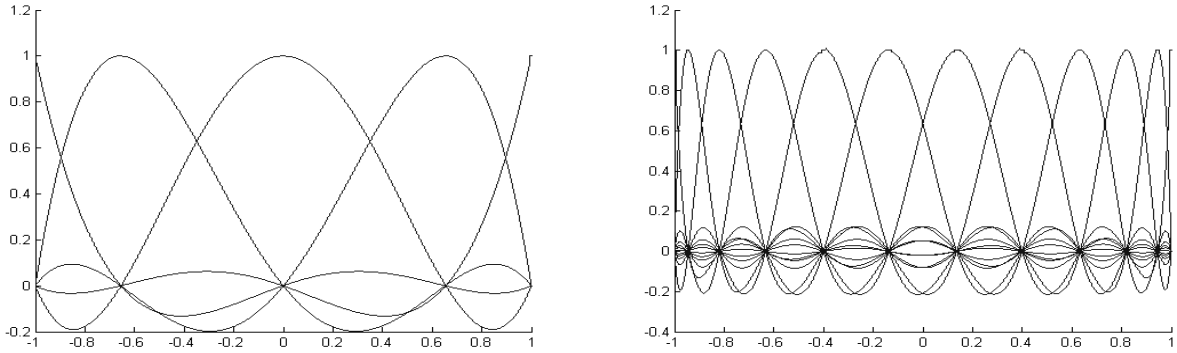

Figure 6: One-dimensional spectral basis functions on a single element for N = 4 (left) and N = 11 (right)

This Eulerian-Eulerian particle tracking method can be functionally implemented into the Nek5000 code to provide a tool for direct numerical simulations of particle fields in many applications. Particle sizes can range to at least 100 nm and are only limited by the physical limitations of the AD equation [18]. These tools can lead towards more accurate and efficient determination of particle deposition patterns for unique geometries with an emphasis on toxic and therapeutic particles in the human respiratory system.

References

1. Gehr, P., F. Blank, and B.M. Rothen-Rutishauser, *Fate of inhaled particles after interaction with the lung surface.* Paediatric Respiratory Reviews, 2006. **7**: p. S73-S75.
2. Singh, N. and G.S. Davis, *Review: occupational and environmental lung disease.* Current Opinion in Pulmonary Medicine, 2002. **8**(2): p. 117-125.
3. Donaldson, K., et al., *The pulmonary toxicology of ultrafine particles.* Journal of Aerosol Medicine-Deposition Clearance and Effects in the Lung, 2002. **15**(2): p. 213-220.
4. Donaldson, K., et al., *Ultrafine particles: mechanisms of lung injury.* Philosophical Transactions of the Royal Society of London Series a-Mathematical Physical and Engineering Sciences, 2000. **358**(1775): p. 2741-2748.
5. Choi, L.T., et al., *Flow and particle deposition patterns in a realistic human double bifurcation airway model.* Inhalation Toxicology, 2007. **19**(2): p. 117-131.
6. Zhang, Z. and C. Kleinstreuer, *Airflow structures and nano-particle deposition in a human upper airway model.* Journal of Computational Physics, 2004. **198**(1): p. 178-210.
7. Fischer, P.F., et al., *Simulation of high-Reynolds number vascular flows.* Computer Methods in Applied Mechanics and Engineering, 2007. **196**(31-32): p. 3049-3060.
8. Zhang, Z. and C. Kleinstreuer, *Transient airflow structures and particle transport in a sequentially branching lung airway model.* Physics of Fluids, 2002. **14**(2): p. 862-880.
9. Weibel, E.R., *Morphometry of the Human Lung*. 1963, New York: Academic Press.
10. Fischer, P.F., *An overlapping Schwarz method for spectral element solution of the incompressible Navier-Stokes equations.* Journal of Computational Physics, 1997. **133**(1): p. 84-101.
11. Chiam, K.H., et al., *Enhanced tracer transport by the spiral defect chaos state of a convecting fluid.* Physical Review E, 2005. **71**(3): p. -.
12. Tufo, H.M. and P.F. Fischer, *Fast parallel direct solvers for coarse grid problems.* Journal of Parallel and

Distributed Computing, 2001. **61**(2): p. 151-177.
13. Witten, M.L., et al., *Acute Cigarette-Smoke Exposure Increases Alveolar Permeability in Rabbits.* American Review of Respiratory Disease, 1985. **132**(2): p. 321-325.
14. Witten, M.L., et al., *New Developments in the Pathogenesis of Smoke Inhalation-Induced Pulmonary-Edema.* Western Journal of Medicine, 1988. **148**(1): p. 33-36.
15. Chaturvedi, A. and Z. Lee, *Three-dimensional segmentation and skeletonization to build an airway tree data structure for small animals.* Physics in Medicine and Biology, 2005. **50**(7): p. 1405-1419.
16. Deville, M.O., P.F. Fischer, and E.H. Mund, *High-Order Methods for Incompressible Fluid Flow*. Cambridge Monographs on Applied and Computational Mathematics, ed. A.I. P.G. Ciarlet, R.V. Kohn, M.H. Wright. 2002: Cambridge University Press.
17. Fischer, P. and J. Mullen, *Filter-based stabilization of spectral element methods.* Comptes Rendus De L Academie Des Sciences Serie I-Mathematique, 2001. **332**(3): p. 265-270.
18. Zhang, Z., et al., *Comparison of micro- and nano-size particle depositions in a human upper airway model.* Journal of Aerosol Science, 2005. **36**(2): p. 211-233.